

*Thieno[2,3-*b*]pyridine derivatives: a new class of antiviral drugs against Mayaro virus*

**Raquel Amorim, Marcelo Damião
Ferreira de Menezes, Julio Cesar Borges,
Luiz Carlos da Silva Pinheiro, Lucio
Ayres Caldas, et al.**

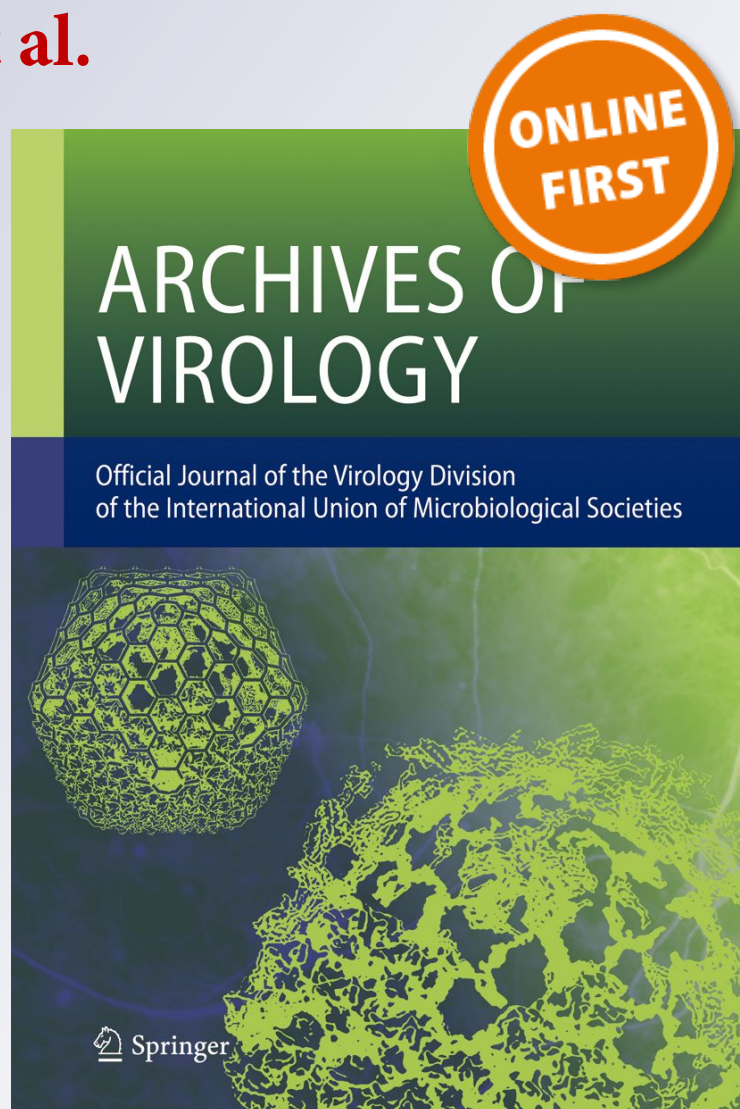
Archives of Virology

Official Journal of the Virology
Division of the International Union of
Microbiological Societies

ISSN 0304-8608

Arch Virol

DOI 10.1007/s00705-017-3261-0



Your article is protected by copyright and all rights are held exclusively by Springer-Verlag Wien. This e-offprint is for personal use only and shall not be self-archived in electronic repositories. If you wish to self-archive your article, please use the accepted manuscript version for posting on your own website. You may further deposit the accepted manuscript version in any repository, provided it is only made publicly available 12 months after official publication or later and provided acknowledgement is given to the original source of publication and a link is inserted to the published article on Springer's website. The link must be accompanied by the following text: "The final publication is available at link.springer.com".

Thieno[2,3-*b*]pyridine derivatives: a new class of antiviral drugs against Mayaro virus

Raquel Amorim¹ · Marcelo Damião Ferreira de Meneses¹ · Julio Cesar Borges² · Luiz Carlos da Silva Pinheiro³ · Lucio Ayres Caldas⁴ · Claudio Cesar Cirne-Santos¹ · Marcos Vinícius Palmeira de Mello⁵ · Alessandra Mendonça Teles de Souza⁶ · Helena Carla Castro⁵ · Izabel Christina Nunes de Palmer Paixão⁷ · Renata de Mendonça Campos¹ · Ingrid E. Bergmann⁸ · Viviana Malirat⁸ · Alice Maria Rolim Bernardino⁹ · Moacyr Alcoforado Rebello¹ · Davis Fernandes Ferreira¹

Received: 25 April 2016 / Accepted: 10 January 2017
© Springer-Verlag Wien 2017

Abstract Mayaro virus (MAYV) is an arthropod-borne virus and a member of the family *Togaviridae*, genus *Alphavirus*. Its infection leads to an acute illness accompanied by long-lasting arthralgia. To date, there are no antiviral drugs or vaccines against infection with MAYV and resources for the prevention or treatment of other alphaviruses are very limited. MAYV has served as a model to study the antiviral potential of several substances on alphavirus replication. In this work we evaluated the antiviral effect of seven new derivatives of thieno[2,3-*b*]pyridine against MAYV replication in a mammalian cell line. All derivatives were able to reduce viral production effectively at concentrations that were non-toxic for Vero cells. Molecular modeling assays predicted low toxicity risk and good oral bioavailability of the substances in humans. One of the molecules, selected for further study, demonstrated a

strong anti-MAYV effect at early stages of replication, as it protected pre-treated cells and also during the late stages, affecting virus morphogenesis. This study is the first to demonstrate the antiviral effect of thienopyridine derivatives on MAYV replication *in vitro*, suggesting the potential application of these substances as antiviral molecules against alphaviruses. Additional *in vivo* research will be needed to expand the putative therapeutic applications.

Introduction

Forest regions have been suffering aggressive deforestation over decades, and a critical outcome of this disruption is the introduction of new arthropod-borne viruses (arboviruses)

✉ Davis Fernandes Ferreira
davisf@micro.ufrj.br

¹ Departamento de Virologia, Instituto de Microbiologia, Centro de Ciências da Saúde, Universidade Federal do Rio de Janeiro, Av. Carlos Chagas Filho, 373, Rio de Janeiro 21941-902, Brazil

² Instituto Federal de Educação, Ciência e Tecnologia do Rio de Janeiro, Campus Nilópolis, Nilópolis 26530-060, Brazil

³ Departamento de Síntese de Fármacos, Instituto de Tecnologia em Fármacos, Farmanguinhos-FIOCRUZ, Rio de Janeiro 21041-250, Brazil

⁴ Laboratório de Ultraestrutura Celular Hertha Meyer, Instituto de Biofísica Carlos Chagas Filho, Universidade Federal do Rio de Janeiro, Av. Carlos Chagas Filho, 373, Rio de Janeiro 21941-902, Brazil

⁵ Laboratório de Antibióticos, Bioquímica, Educação e Modelagem Molecular, Universidade Federal Fluminense, Campus Valonguinho, Outeiro de São João Batista s/n°, Niterói, Rio de Janeiro 24020-150, Brazil

⁶ Laboratório de Modelagem Molecular e QSAR, Faculdade de Farmácia, Universidade Federal do Rio de Janeiro, Rio de Janeiro, RJ CEP 21941-590, Brazil

⁷ Laboratório de Virologia Molecular e Biotecnologia Marinha, Programa, Departamento de Biologia Celular e Molecular, Instituto de Biologia, Universidade Federal Fluminense, Niterói, Brazil

⁸ Centro de Virología Animal (CEVAN), Instituto de Ciencia y Tecnología Dr. César Milstein, Consejo Nacional de Investigaciones Científicas y Técnicas (CONICET), Saladillo 2468, CP: 1440 Buenos Aires, Argentina

⁹ Departamento de Química Orgânica, Instituto de Química, Universidade Federal Fluminense, Outeiro de São João Batista, s/n, Centro, Niterói, Rio de Janeiro 24020-141, Brazil

into new ecological niches. Urban areas are now providing ideal conditions for the establishment of several etiological agents responsible for many medically important diseases. About 200 arboviruses have been isolated in Brazil and about 40 of these cause diseases in humans. Amongst them, Dengue virus (DENV), and more recently Zika (ZIKV), and Chikungunya (CHIKV) viruses have caused a profound impact on the public health system in Brazil, triggering a worldwide alert [1]. It has been suggested that following the same trend, other arboviruses may emerge as they are introduced into urban areas and then transmitted by the highly anthropophilic *Aedes* genus [2].

Mayaro virus (MAYV), closely related to CHIKV and other alphaviruses produces an acute, self-limited dengue-like illness that is accompanied by long-lasting arthralgia [3]. In forest areas, mosquitoes of the *Haemagogus* genus transmit MAYV, but urban mosquitoes from the *Aedes* genus can also propagate the virus [4], therefore, the potential spread of MAYV is of significant concern. MAYV has been isolated in Colombia, Venezuela, French Guiana, Suriname, and the United States and cases of imported infections have been reported in France, Holland, Switzerland and Germany [5]. More recently in Brazil, six cases of Mayaro fever have been identified in co-circulation with dengue virus in the state of Mato Grosso, and over 30 cases were reported in the state of Goiás [6].

Currently, there is no licensed vaccine or antiviral treatment against MAYV [2]. Therefore, the search for antiviral drugs against MAYV and other pathogenic arboviruses is of great importance. MAYV has served as a model for the study of the antiviral activity of several substances on alphavirus replication, such as weak bases [7], prostaglandins [8], brefeldin [9], monensin [10], pyrazolo/pyridine compounds [11], quercetin [12] and *Cassia australis* extracts [13].

It has also been shown that derivatives of the thienopyridine system present many biological activities, mainly directed against proteins involved in cell proliferation and tumor development [14, 15]. As changes in cell proliferation are induced by a variety of viruses to promote viral replication, several studies correlate antitumor activity with antiviral activity in heterocyclic molecules [16]. Thienopyridine derivatives induce coronary endothelium cells to release nitric oxide [17], which is an important cell signaling molecule with antimicrobial activity against bacteria, protozoa and some viruses [18]. Recently, new derivatives of the thieno[2,3-*b*]pyridine system were synthesized and shown to present giardicidal activity [11]. These derivatives are structurally related to molecules with reported antiviral activity [19, 20]. Therefore, study on the antiviral activity of thienopyridine derivatives is a promising field. The aim of the current work was to evaluate the antiviral activity of synthetic thienopyridine

derivatives against MAYV *in vitro*, and to perform preliminary studies for their potential use as antiviral drugs.

Material and methods

Cells and viruses

African green monkey kidney (Vero) cells were obtained from the Pan American Health Organization (Rio de Janeiro, Brazil). Cells were grown in Dulbecco's Modified Eagle's Medium (DMEM, Gibco) supplemented with 5% bovine fetal serum (FBS, Gibco), 0.23% NaHCO₃, 0.0025 mg/mL amphotericin B (Fungizone, Gibco), 500 U/mL penicillin and 0.1 mg/mL streptomycin. The cells were maintained at 37 °C and 5% CO₂ atmosphere. MAYV was obtained from American Type Culture Collection (ATCC VR 66, strain TR 4675). Viruses were propagated in Vero cells, and virus titers were determined by plaque assay [21].

Pyridine derivatives

Synthesis of the thieno[2,3-*b*]pyridine derivatives, as well as the first studies on their biological activities, are published elsewhere [11]. The structures of these derivatives are presented in Fig. 1. All derivatives differ only in the nature (H, -CH₃, -NO₂ and -F) and position (para or meta) of the radical in the phenyl ring. The molecules were synthesized by the Laboratório de Síntese de Heterociclos from the Universidade Federal Fluminense (UFF), maintained at 50mM in DMSO and stored at -20 °C. Ribavirin was obtained from Sigma-Aldrich, US.

Cytotoxicity assay

Cytotoxicity of the thienopyridine derivatives on Vero cells was tested *in vitro* using the neutral red dye uptake method [22]. Briefly, 2 x 10⁴ Vero cells were seeded into each well of a 96-well plate and were incubated for 24 hours at 37°C with different concentrations (from 3.125 to 800 μM) of

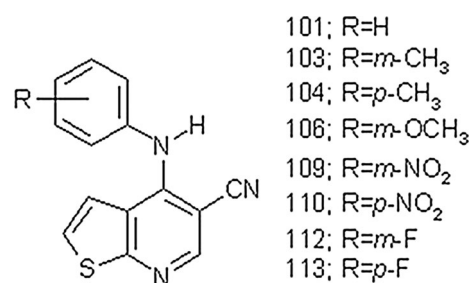


Fig. 1 Structures of the thieno[2,3-*b*]pyridine-5-carbonitrile derivatives

each test molecule, diluted in DMEM (containing 2% fetal serum). After this period, cells were then rinsed with PBS and incubated for 3 hours with 0.05% neutral red solution prepared in serum-free DMEM. Next, cells were rinsed a second time and fixed with 20% paraformaldehyde for 5 minutes. The incorporated dye was extracted with 50% methanol and 1% acetic acid for 20 minutes, and the resulting optical density of the solution was determined at 490 nm wavelength using a microplate reader. Cells treated with DMSO (0.4%) in DMEM were used as a control. The relative cell viability was calculated as a percentage comparing treated to mock-treated cells. Concentrations that maintained greater than 90% cell viability after treatment were considered non-toxic [22].

Infectious virus TCID₅₀ assay

To evaluate whether thienopyridines molecules affect the replication of MAYV, 2×10^5 Vero cells were seeded into each well of a 24-well plate the day before infection. The virus inoculum was diluted to a multiplicity of infection (MOI) of 0.05 in DMEM without serum. After 1 hour of adsorption at 37 °C, virus inoculum was removed by aspiration, cells were washed with PBS to remove unbound viruses, and fresh medium was added with the indicated concentration of the compound. Infected cells were also treated with culture medium containing 1% DMSO to determine the residual antiviral effect of the vehicle, and 200 µM of Ribavirin as a positive control for antiviral activity. After 24 hours of incubation at 37 °C, the culture medium was collected, and infectious virus yield in the cell supernatant was determined by titration using the TCID₅₀ assay in Vero cells [23].

Metabolic labeling of proteins

2×10^5 Vero cells cultivated in Kimble flasks (Thomas Scientific, USA) were infected with MAYV at an MOI of 1.0. After 1 hour of adsorption, the inoculum was aspirated and culture media containing 100 µM of the substance 104 was added to the cells, with incubation then allowed to proceed for 6 hours. Cells were then washed with PBS prior to starvation in DMEM without L-cysteine and L-methionine for 1 hour. After this period, the starvation medium was supplemented with 60 uCi/mL [³⁵S] methionine and cells were incubated for an additional hour. Cells were then washed with PBS and lysed in 80 µL of loading buffer (0.08M pH 6.8 Tris-HCl, 10% glycerol, 2.3% SDS, 0.002% bromophenol blue and 5% β-mercaptoethanol). The cell proteins were analyzed by SDS-PAGE as described by Laemmli [24]. Gel slabs were autoradiographed with Kodak X-Omat K film. MAYV proteins were identified by estimation of their molecular weight as

compared to reference protein standards. Densitometry quantification of each band was determined by ImageJ version 1.49 software analysis.

Time of addition assay

To determine which stage of the viral life cycle was affected by the drug, the effects of simultaneous treatment, pre-treatment and post-treatment were evaluated. Monolayers of Vero cells grown in 24-well plates, as previously described, were infected with MAYV at an MOI of 0.05 at time zero. Cells were treated with the drug (substance 104 diluted in culture medium) to a final concentration of 100 µM for 1, 2 or 3 hours before infection ($t = -1, -2$ and -3) to evaluate pre-treatment effects, at the moment of viral adsorption at 37 °C ($t = 0$), for simultaneous treatment, and at 1, 2 or 3 hours after virus adsorption ($t = 1, 2$ and 3), to evaluate post-treatment conditions. The cells were incubated at 37 °C for 5 hours after adsorption, when the supernatants were collected. All virus titers were determined for each treatment by plaque forming assay on Vero cells. Briefly, after 1 hour of adsorption at 4 °C, cells were washed three times with PBS and overlaid with 3% carboxymethylcellulose in culture medium. After 72 hours of incubation at 37 °C, cells were fixed with 20% formaldehyde for 2 hours and stained with crystal violet for 5 minutes. The plaques formed after each treatment were counted and the titer calculated.

Measurement of virucidal activity

To evaluate whether substance 104 has a direct effect on virus infectivity, approximately 250 plaque forming units of MAYV were incubated at 37 °C in DMEM containing the drug at the indicated concentrations. As a control, the same amount of virus was incubated in DMEM containing 1% DMSO. The remaining virus titer obtained after each treatment was determined by plaque assay on Vero cells, as described above.

Attachment assay

Vero cell monolayers grown in 6-well plates were pre-chilled at 4 °C for 10 minutes and infected with MAYV diluted in medium to approximately 250 PFU per well, in the absence or presence of substance 104 at a final concentration of 100 µM. After 1 hour of adsorption at 4 °C, the unabsorbed virus was removed by washing the monolayer with cold PBS and then cells were overlaid with 3% carboxymethylcellulose in culture medium. After 72 hours, cells were fixed with 20% formaldehyde for 2 hours and stained with crystal violet for 5 minutes. The plaques formed after each treatment were counted and the titer calculated.

Transmission electron microscopy

2 x 10⁶ Vero cells grown in 25 cm² flasks were infected with MAYV at an MOI of 0.05. After 1 hour of adsorption, cells were treated with 100 μM of substance 104 and incubated at 37 °C for 8 hours. The monolayers were then fixed and processed for transmission electron microscopy using standard methods. Briefly, cells were fixed in 2.5% glutaraldehyde in 0.1 M cacodylate buffer, pH 7.2, and afterwards treated with 1% OsO₄ in 0.1 M cacodylate buffer pH 7.2 plus 0.8% potassium ferrocyanide for 1 hour. Samples were then dehydrated in ethanol and flat embedded in Polybed (Polysciences®). Ultrathin sections were stained with 5% uranyl acetate and lead citrate and observed using a Zeiss 900 transmission electron microscope. The number of nucleocapsids in each condition was determined by ImageJ version 1.49 software analysis.

Molecular modeling

All molecular modeling calculations were performed using the SPARTAN'10 program (Wavefunction Inc.). Molecular structures were submitted in neutral states for conformational analysis using Merck Molecular Force Field (MMFF). The derivatives in their minimum energy conformation were subjected to a geometry optimization in a vacuum using the semi-empirical method PM6. To evaluate the electronic properties, they were submitted to a single-point calculation DFT B3LYP/6-31G* basis set. Subsequently, the structural and electronic properties of all structures were calculated, including Highest Occupied Molecular Orbital (HOMO) and the Lowest Unoccupied Molecular Orbital (LUMO) energy, orbital coefficient and density, dipole moment and MEP maps (molecular electrostatic potential). The three-dimensional isosurfaces of the MEPs at the van der Waals contact surface represent electrostatic potentials superimposed onto a surface of constant electron density (0.002 e/au³) and were generated at a range of -70 to +100 kcal/mol. These color-coded isosurface values provide an indication of the overall molecular size and location of negative (red) or positive (blue) electrostatic potentials.

The pharmacokinetic profile of the thieno[2,3-*b*]pyridine derivatives, critical for a compound's oral bioavailability, was also evaluated according to Lipinski's 'rule-of-five' [25]. Further, the ADMET risk score, which computes parameters like lipophilicity, permeability, hydrogen bonding and toxicities values, was calculated using the ADMET Predictor™ (Simulations Plus Inc., Lancaster, CA, USA). As a control, we used ribavirin, an antiviral drug.

Statistical analysis

All experiments were performed in triplicate, and the data are presented as mean ± standard deviation (SD). A two-tailed p-value of < 0.05 in a Students *t*-test, comparing sets of data, was considered to be statistically significant. GraphPad Prism 6 was used to conduct statistical analyses and to create graphs.

Results

Cytotoxicity assay

Cell viability in the presence of thienopyridine compounds was assayed through use of the neutral red dye uptake method. As a comparison, we used the broad spectrum antiviral ribavirin, that has also been shown to have antiviral activity against alphaviruses [26]. As shown in Table 1, there was a remarkable difference in cytotoxicity for the two isomers with a methyl motif, making the para-substituted molecule (104) 5 times less toxic than its isomer (103). In fact, molecule 104 (*p*-CH₃) presented the lowest cytotoxicity of all tested derivatives, including a lower cytotoxicity in Vero cells than ribavirin. Regarding the nitrite isomers, the para-substituted molecule (110) was about 2 times less toxic than the meta-substituted isomer (109), and both presented lower cytotoxicity to Vero cells than ribavirin. Finally, both fluorine molecules (112 and 113) were more toxic to Vero cells than ribavirin and had the largest differences in toxicity depending on the fluorine position. The meta-substituted molecule (112) is almost six times less toxic than the 113 isomer (para-substituted). Treatment with 100 μM of molecules 103, 104 and 110, 50

Table 1 Effect of thieno[2,3-*b*]pyridine derivatives on Vero cell viability and replication of MAYV

Molecule	R	*CC ₅₀ (μM)	**IC ₅₀ (μM)	***SI
101	H	302.1 ± 21.2	11.7 ± 3.8	25.8
103	<i>m</i> -CH ₃	450 ± 8.0	20.1 ± 2.6	22.4
104	<i>p</i> -CH ₃	2500 ± 17.8	20.0 ± 2.9	125.0
109	<i>m</i> -NO ₂	760 ± 19	17.9 ± 2.3	42.4
110	<i>p</i> -NO ₂	1400 ± 90	69.5 ± 8.8	20.1
112	<i>m</i> -F	400 ± 3.4	9.4 ± 1.1	42.5
113	<i>p</i> -F	68.84 ± 3.3	>10	<6.88
Ribavirin		523.4 ± 42.3	62.5 ± 4.5	8.37

* CC₅₀ - Concentration of the compound capable of reducing cell viability by 50%; ** IC₅₀ - Concentration of the compound capable of reducing the virus yield by 50%, when compared to control cells; *** SI - Selectivity Index (CC₅₀/ IC₅₀). SI values were obtained from data obtained in cytotoxicity and antiviral assays and are expressed as concentration (μM) ± SD

μM of molecule 109 and $10 \mu\text{M}$ of molecules 112 and 113 (below the CC_{50} value) did not result in a significant difference in cell morphology and viability as measured by the neutral-red dye uptake assay (data not shown), when compared to mock-treated cells. Therefore, lower concentrations, than the ones referred to above for each drug, were selected for the virus yield assay.

Molecular modeling

A molecular modeling approach was used to investigate physicochemical properties of the thieno[2,3-*b*]pyridine derivatives that could explain the different cytotoxicity and antiviral activities presented in Table 1. To obtain the lowest energy conformer, we carried out a conformational analysis for each derivative by MMFF, where only the best conformer (lowest energy) was kept. Results indicate that the presence of the electron-withdrawing groups $-\text{NO}_2$ and $-\text{F}$ causes an increase in activity when the substitution occurs at the meta position of the ring (Table 2). The overall analysis of HOMO and LUMO energies revealed that electronegative groups cause a decrease in the values of LUMO although both energies had no direct correlation

with the antiviral activity (Table 2). Likewise, the dipole did not reveal further clues about the biological profile of these derivatives (data not shown). The MEP maps (Fig. 2) of derivatives 109 (*m*- NO_2) and 110 (*p*- NO_2) present the most evident differences in the electronic profile.

The pharmacokinetic profile is crucial for a compound's oral bioavailability and was evaluated according to Lipinski's 'rule-of-five'. This method analyzes features that a drug should present to allow absorption and permeability across membranes (i.e., molecular weight ≤ 500 Da, $\text{cLog P} \leq 5$, the number of hydrogen-bond acceptors (nHBA) ≤ 10 , and the number of hydrogen-bond donors (nHBD) ≤ 5 [25]). As shown in Table 3, our results indicate that all thieno[2,3-*b*]pyridine derivatives fulfill these rules, suggesting that these derivatives are potential drug candidates with good oral bioavailability and low cytotoxicity.

Finally, the thieno[2,3-*b*]pyridine derivatives were submitted to *in silico* ADMET and toxicity risk analysis using the Osiris Property Explorer program. As a control, we used ribavirin, a drug already used in the market as a broad-spectrum antiviral [26]. The ADMET Risk is a score in the 0 to 24 range that indicates the number of potential problems of absorption, distribution, metabolism, excretion and toxicity a compound might have. The toxicity risk is a score in the 0 to 7 range that indicates the number of potential toxicity problems a compound might have, including mutagenic, tumorigenic, irritant and reproductive issues. The toxicity and ADMET risk analysis showed that the molecules 101, 103, 104, 109 and 110 had scores similar to ribavirin. Interestingly, compounds 112 and 113 had the lowest risk (Fig. 3).

The preliminary results obtained with these thienopyridine derivatives as potential antiviral compounds encouraged us to perform further studies on different stages of the virus infection cycle, with one molecule selected because of its very low toxicity and strong antiviral activity, namely drug 104.

Table 2 Putative molecular stereoelectronic properties (HOMO energy (E_{HOMO}), LUMO energy (E_{LUMO}) of the thieno[2,3-*b*]pyridine derivatives

Molecule	E_{HOMO} (eV)	E_{LUMO} (eV)
101	-5.93	-1.33
103	-5.89	-1.29
104	-5.98	-1.13
109	-6.32	-2.44
110	-6.43	-2.38
112	-6.02	-1.56
113	-5.97	-1.34

Fig. 2 Molecular Electrostatic Potential map (MEP) of the thieno[2,3-*b*]pyridine-5-carbonitrile derivatives. The color-coded isosurface values provide an indication of the overall molecular size and location of negative (red) or positive (blue) electrostatic potentials (color figure online)

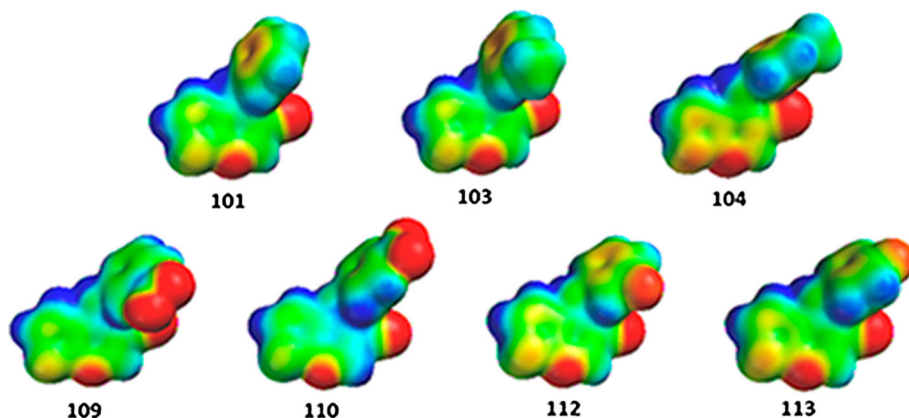


Table 3 Analysis of lipophilicity (cLog P), molecular weight (MW), number of hydrogen bond donor groups (HBD) and number of hydrogen bond acceptor group (HBA) parameters, according to Lipinski's 'rule of 5'

Molecule	HBD	HBA	cLogP	MW
101	1	4	3.58	251.31
103	1	4	3.89	265.34
104	1	4	3.89	265.34
109	1	7	3.45	296.31
110	1	7	3.45	296.31
112	1	4	3.64	269.30
113	1	4	3.64	269.30

Virus yield assay

Evaluation of antiviral effect was carried out in Vero cells. Vero cells were infected with MAYV using a multiplicity of infection of 0.05 and treated for 24 hours with increasing concentrations of the substances. The TCID₅₀ method was used to titrate virus yield, and the concentration capable of reducing the virus yield by 50% (IC₅₀) was obtained from a dose-response graph and is presented in Table 1. Ribavirin was used as a control.

Results showed that concentrations of the molecules ranging from >10 to 69.5 μ M led to a significant reduction of infective viral yields, when compared to mock treatment, and that the inhibitory effect was dose-dependent (Table 1 and data not shown). The cytotoxicity and antiviral effect of derivative 104 are shown in detail in Fig. 4A. Cytotoxicity was lower than 20% at all tested concentrations (Fig 4A, open squares), whereas viral yield was reduced in a dose-dependant fashion (Fig 4A, black circles). Selectivity

indexes (ratio CC₅₀/IC₅₀) were determined for each molecule, rendering values from < 6.88 to 125 unit (Table 1), the latter one obtained for molecule 104, which was the drug presenting the best selectivity index.

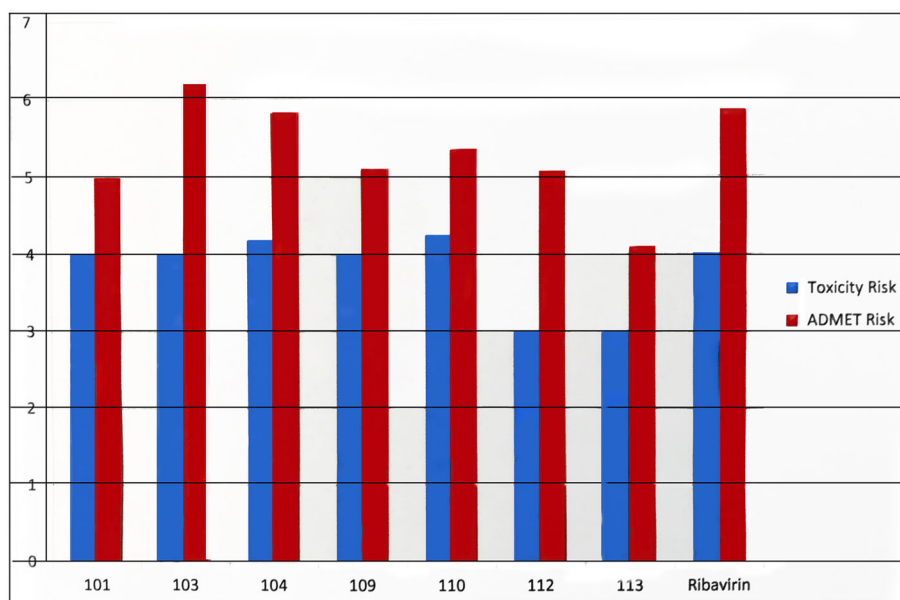
Metabolic labeling of proteins

To evaluate the effect of the 104 molecule on viral protein synthesis, Vero cells were infected, and *de novo* synthesized proteins were labeled with ³⁵S-methionine. A severe shut-off in cellular protein synthesis was observed in infected cells, a well-documented feature of Alphavirus infections [27] (Fig. 4B, compare lanes 1 and 2 with 3 and 4). The viral protein precursors p62 and p130 and the viral proteins E1 and E2 were not detected in 104 treated cells (Fig. 4B, lane 2). Treatment with the 104 molecule also led to a 3-fold reduction in capsid protein synthesis when compared to control infected cells (Fig. 4B, compare lanes 1 and 2).

Time of addition assay

To address which stage of virus replication was affected by drug 104, we added the molecule before, during and after the addition of virus to the cells and measured the production of infectious virus by plaque assay (Fig. 5). Ribavirin was used as control as is known its antiviral action occurs at the viral RNA replication stage. As result, we observed that ribavirin has no antiviral effect when added 3 hours before infection, and its antiviral action is potentiated when it is added immediately before, simultaneously or after viral adsorption (Fig. 5). For drug 104, a strong inhibitory effect was observed when the drug was added before or simultaneously with the viral inoculum ($t = -3$ to 0). When the molecule was added one

Fig. 3 Toxicity risk assessment and ADMET risk of the thieno[2,3-*b*]pyridine-5-carbonitrile derivatives



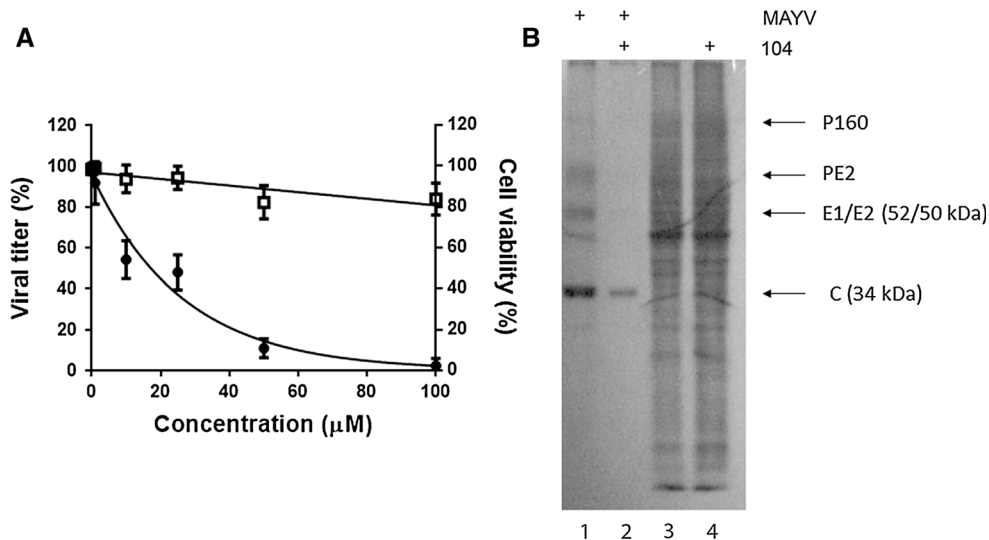


Fig. 4 Cytotoxicity and antiviral effect of drug 104. A. Circles: Monolayers of Vero were infected with MAYV at an MOI of 0.05 and treated with drug 104 at different concentrations. After 24 hours of incubation, supernatants were harvested and viral titer was determined by TCID50 assay. Results present percentage of viral titer obtained under each condition, when compared to untreated cells. Open squares: Monolayers of Vero cells were treated with drug 104 at different concentrations. After 24 hours of incubation, cells were stained with neutral red. Results present the percentage of viable cells

under each condition, when compared to untreated cells. B. Vero cells were infected with MAYV treated or untreated with drug 104 at a concentration of 100 μM. Non-linear curve regression fits for each set of data are represented by black lines. *De novo* synthesized proteins were labeled with [³⁵S]-methionine. Samples were processed by SDS-PAGE, followed by autoradiography. P160: precursor of structural proteins; PE2, precursor of E2 glycoprotein; E1, mature E1 glycoprotein; E2, mature E2 glycoprotein

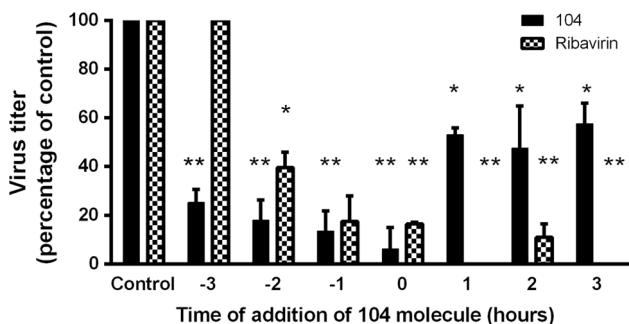


Fig. 5 Effect of the addition of drug 104 on MAYV replication over time. Monolayers of Vero cells were infected with MAYV at an MOI of 0.05 at time zero. At the times indicated, drug 104 or ribavirin was added to a final concentration of 100 μM or 200 μM, respectively. Cells were incubated at 37 °C for 5 hours whereupon the supernatants were collected and virus titer was determined by plaque forming assay in Vero cells. Data are presented as percentage of virus titer, when compared to control cells and are expressed as the mean of three experiments ± standard error. Statistical analysis was performed using the t-student's test: * p < 0.05; **p < 0.01

hour after virus infection (t = 1-3); however, this inhibition only reached about 50%, when compared to the control.

Virucidal assay

To evaluate the direct effect of drug 104 on MAYV replication, a virucidal assay was performed. We observed a 50% reduction in virus titer after treatment with 100 μM of drug 104 for 1

hour when compared to the virus titer obtained after incubation of the viral inoculum with culture medium without the substance, under the same conditions (Fig. 6A and B). When the effect was evaluated at different incubation times (20, 40 and 60 minutes), it was observed that significant virucidal effect could be demonstrated only after 60 minutes of incubation (Fig. 6C). Additionally, this effect was only observed at concentrations of over 25 μM, approximately (Fig. 6D)

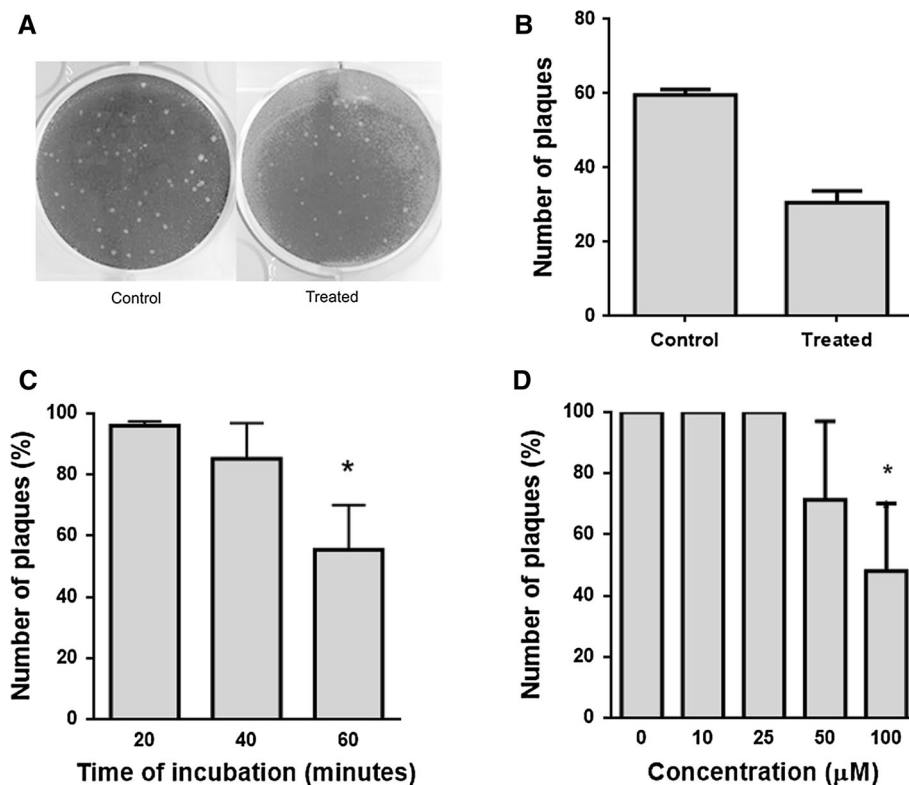
Attachment assay

To evaluate the putative effect of molecule 104 during the early steps of virus replication, we studied whether this thienopyridine derivative could interfere with viral adsorption, measured by assessing any effect on virus production. Our results show that no significant differences were detected in virus yield when Vero cells were infected with MAYV pre-treated at 4 °C in the presence or absence of 100 μM of molecule 104, (Fig. 7), indicating that treatment did not interfere with viral adsorption.

Transmission electron microscopy

Previously (Fig. 5), we had observed that a certain level of inhibition was maintained even when the 104 molecule was added later in infection, indicating that one of the targets for this antiviral drug may be late events in viral

Fig. 6 Virucidal activity of the 104 molecule. **A.** MAYV was incubated (at 37 °C for one hour) in the absence or presence of derivative 104 at 100 μ M. The remaining virus titer was determined by plaque assay; the figure is a representative result from three independent experiments. **B.** Quantification of plaques shown in A. **C.** MAYV was incubated with 100 μ M of derivative 104 at 37 °C for 20, 40 or 60 minutes (bar graph). **D.** MAYV was incubated in the absence or presence of the derivative 104 at 10, 25, 50 100 μ M, at 37 °C for one hour. The remaining virus titer was determined by plaque assay. Statistical analysis was performed using t-student's test: * $p < 0.05$



replication. Therefore, we addressed the effect of this drug on the assembly and budding steps of MAYV by using transmission electron microscopy of Vero cells infected with MAYV and treated with drug 104. We observed a reduction in the number of intracytoplasmic nucleocapsids and the number of mature virus particles in treated cells (231.7 ± 52.8) (Fig. 8D and F) when compared to control cells (450.0 ± 90.0) (Fig. 8A and B). In treated cells, we also visualized particles that do not seem to assemble correctly, as in Fig. 8E, where a group of

three nucleocapsids covered by the same membrane is observed. Finally, we also observed viral mRNA transcription centers (type 1 cytopathic vacuoles) in control and treated cells (Fig. 8C and G), indicating the apparently normal establishment of transcription centers in treated cells.

Discussion

In this study, we investigated the *in vitro* antiviral activity of thienopyridine derivatives against MAYV. Recent introduction into urban areas of the arboviruses ZIKV and CHIKV has had a substantial impact on public health and raised concerns about other viruses also transmitted by *Aedes* mosquitoes, such as MAYV [2]. Therefore, our findings may contribute to the development of an effective control strategy against MAYV infection.

Our results indicated that the position of the motifs in the thienopyridine derivative's phenyl group is an important factor in determining molecular cytotoxicity. However, we are not able to affirm which position leads to lower cytotoxicity or what type of radical is less cytotoxic (Table 1), suggesting that the whole structure of the molecule may be necessary for determining cytotoxicity. Moreover, our results showed that this basic structure may be promising in studies using mammalian cells due to its low toxicity. Except for one molecule (113), all the isomers

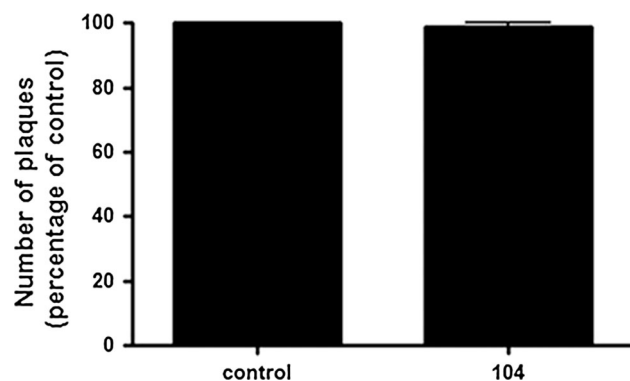


Fig. 7 Effect of derivative 104 on viral adsorption. Vero cells were infected with MAYV at 4 °C in the presence or absence of the drug 104 at 100 μ M. Virus adsorption was determined by plaque assay. The values correspond to the percentage of virus titer in each treatment, compared to control cells, and are expressed as the mean of three experiments \pm standard error

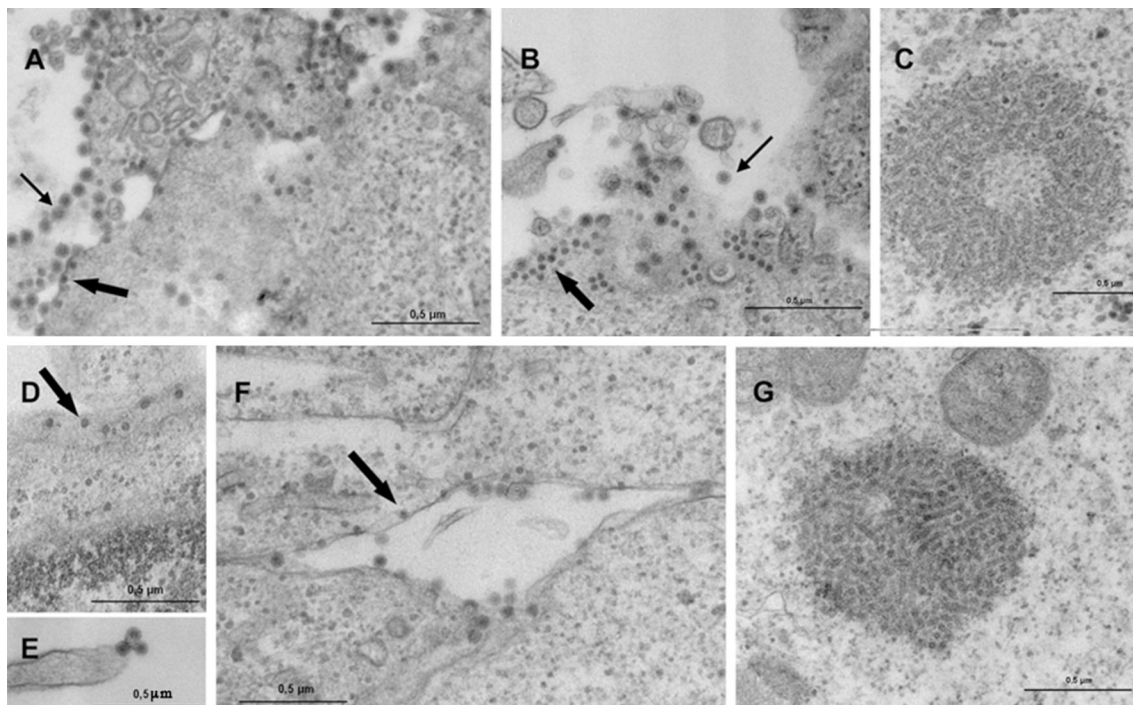


Fig. 8 Effect of derivative 104 on viral morphogenesis: Confluent Vero cells grown in 25 cm² flasks were infected with MAYV at an MOI of 0.05. After adsorption, the cells were treated with drug 104 at a final concentration of 100 μM and incubated at 37 °C for 8 hours. The monolayers were then fixed and processed for transmission

electron microscopy using standard methods. Photos A, B, and C: Cells infected with MAYV; Photos D, E, F and G: Cells infected with MAYV and treated with drug 104 at 100 μM. Thin arrows: Free viral particles; Thick arrows: nucleocapsids. Scale bars: 0.5 μm

presented lower or similar toxicity when compared to ribavirin, which has been shown to have a broad spectrum of antiviral action. Ribavirin is known to inhibit the replication of Chikungunya virus, which is another member of the *Togaviridae* family [26]. The *in vitro* cytotoxicity tests were corroborated by *in silico* analysis, as shown in Table 2. The substances used in this study are presumed to have good oral bioavailability according to the Lipinski's 'Rule-of-five' [25] and have toxicity risks similar or lower than an already approved antiviral drug ribavirin (Fig. 3). Altogether, our results suggest that the thienopyridine derivatives are suitable candidates for a new class of antiviral drugs with a low risk of toxicity. These drugs warrant further study *in vivo*.

With regard to the antiviral activity, except for drug 113, all isomers had significant and even more potent antiviral activity than ribavirin. All the motif isomers had similar antiviral activities, except the nitro derivatives 109 (*m*-NO₂) and 110 (*p*-NO₂), as shown in Table 1. This difference could be explained by the results of the MEP maps (Fig. 2), which showed that these derivatives present the most distinct electronic profile. Moreover, the nitro substituent is a strong electron-withdrawing group that completely changes the properties of the molecule, reducing the electron density in the ring. This may explain the reduced

biological activity of the 110 compound. Derivatives with fluorine substituent have high antiviral activity (112 and 113) which can be related to hydrogen bonds formed by a fluorine atom and the drug target.

Metabolic labeling of the viral proteins demonstrated that the synthesis of these proteins is severely impaired in cells treated with drug 104 (Fig. 4B). Despite inhibiting virus replication, cellular protein synthesis was not reestablished under our experimental conditions. The protein synthesis shut-off observed in vertebrate cells infected with alphaviruses results from inhibition of transcription caused by the viral nonstructural protein nsP2, and inhibition of translation caused by activation of PKR through the detection of viral dsRNA. There is also evidence that the subgenomic viral RNA, which codes for the structural proteins, and the capsid protein itself also inhibits host cell translation [28, 29]. As the capsid protein is still detected in treated cells (Fig. 4, lane 2), it could still be available to induce the observed arrest in translation.

Several studies have demonstrated that molecules can interfere with viral adsorption by blocking viral receptors [30]. The adsorption of alphaviruses at the cell surface is a process that depends on the interaction between viral glycoproteins (especially E2) and cellular receptor(s). The

time of addition assay (Fig. 5) suggests that drug 104 possibly affects early events during virus infection. Ribavirin was used as a control, as its antiviral action is characterized by the inhibition of viral RNA synthesis. As expected, ribavirin has no antiviral effect when added 3 hours before infection; its antiviral action only starts when added immediately before, simultaneously or after viral adsorption (Fig. 5). In contrast, it was observed that the drug 104 inhibits viral replication more potently when added before the viral inoculum, and this inhibition is partially lost when it is added at later times of infection. The difference in behavior visualized when molecule 104 and Ribavirin are added at different times prior or after infection indicate that these molecules have distinct modes of action, and that early stages of viral infection are the target for drug 104, as well as other later stages in viral production. This possibility is supported by the results from the virucidal activity assays (Fig. 6), since low concentrations that strongly inhibited virus replication in cell culture had no significant virucidal effect. Furthermore, long incubation times of the virus with the drug were required, and it would be very unlikely for the drug and virus to maintain prolonged contact during natural infection. Moreover, our results also indicate that thienopyridine treatment does not interfere directly with viral adsorption (Fig. 7), indicating that the early stages of infection affected by the treatment are post-entry events. The transmission electron microscopy images (Fig. 8) indicate that some degree of MAYV assembly and budding deficiency takes place after drug treatment, mainly during envelopment, which may favor the production of noninfectious virus particles.

Conclusions

This work is the first to demonstrate the antiviral effect of thienopyridine derivatives on MAYV replication, affecting early and late stages, in particular morphogenesis. Our results suggest the potential application of these substances as a new class of antiviral drugs, with low cytotoxicity and good predicted bioavailability. These thienopyridine derivatives show potential applicability for use as antiviral therapeutics against alphaviruses.

Acknowledgements We thank CAPES, FAPERJ and INBEB/CNPq for their financial support. This work was supported by The National Institute of Structural Biology and Bioimages INBEB/CNPq – Grant no. 57.3767/2008-4) and Fundação de Amparo à Pesquisa do Estado do Rio de Janeiro (FAPERJ Edital 26/2013 110.034/2014 and FAPERJ APQ1 no.E26/110.370/2012); Raquel Amorim was supported with a Masters scholarship from the Coordenação de Aperfeiçoamento de Pessoal de Nível Superior (CAPES).

Conflict of interest The authors declare that they have no competing interests.

Authors' contributions RA carried out the cytotoxicity, antiviral, attachment and time of addition assays and drafted the manuscript. JCB and LCSP participated in the analysis of the derivatives chemical characteristics. LAC carried out the electron microscopy assay. MDFM, AMRB, MAR, INCPP and DFF conceived the study, contributed to its design and coordination, and to the drafting of the manuscript. IEB and VM also contributed to the study design and the manuscript review. AMTS and MVPM calculated the structure-activity relationship using the molecular modeling approach. HCC carried out the *in silico* ADMET evaluation. All authors read and approved the final manuscript.

References

1. Marcondes CB, Ximenes MF (2015) Zika virus in Brazil and the danger of infestation by *Aedes* (Stegomyia) mosquitoes. *Rev Soc Bras Med Trop*. doi:10.1590/0037-8682-0220-2015
2. Figueiredo ML, Figueiredo LT (2014) Emerging alphaviruses in the Americas: Chikungunya and Mayaro. *Rev Soc Bras Med Trop* 47(6):677–683. doi:10.1590/0037-8682-0246-2014
3. Tesh RB, Watts DM, Russell KL, Damodaran C, Calampa C, Cabezas C, Ramirez G, Vasquez B, Hayes CG, Rossi CA, Powers AM, Hice CL, Chandler LJ, Cropp BC, Karabatsos N, Roehrig JT, Gubler DJ (1999) Mayaro virus disease: an emerging mosquito-borne zoonosis in tropical South America. *Clin Infect Dis* 28(1):67–73. doi:10.1086/515070
4. Long KC, Ziegler SA, Thangamani S, Hausser NL, Kochel TJ, Higgs S, Tesh RB (2011) Experimental transmission of Mayaro virus by *Aedes aegypti*. *Am J Trop Med Hyg* 85(4):750–757. doi:10.4269/ajtmh.2011.11-0359
5. Vasconcelos PF, Calisher CH (2016) Emergence of human arboviral diseases in the Americas, 2000–2016. *Vector Borne Zoonotic Dis* 16(5):295–301. doi:10.1089/vbz.2016.1952
6. Vieira CJ, Silva DJ, Barreto ES, Siqueira CE, Colombo TE, Ozanic K, Schmidt DJ, Drummond BP, Mondini A, Nogueira ML, Bronzoni RV (2015) Detection of Mayaro virus infections during a dengue outbreak in Mato Grosso, Brazil. *Acta Trop* 147:12–16. doi:10.1016/j.actatropica.2015.03.020
7. Ferreira DF, Santo MP, Rebello MA, Rebello MC (2000) Weak bases affect late stages of Mayaro virus replication cycle in vertebrate cells. *J Med Microbiol* 49(4):313–318
8. Burlandy FM, Rebello MA (2001) Inhibition of Mayaro virus replication by prostaglandin A(1) in Vero cells. *Intervirology* 44(6):344–349 (pii: int44344)
9. Da Costa LJ, Rebello MA (1999) Effect of brefeldin A on Mayaro virus replication in *Aedes albopictus* and Vero cells. *Acta Virol* 43(6):357–360
10. De Campos RM, Ferreira DF, Da Veiga VF, Rebello MA, Rebello MC (2003) Effect of monensin on Mayaro virus replication in monkey kidney and *Aedes albopictus* cells. *Acta Virol* 47(2):113–119
11. Bernardino AM, da Silva Pinheiro LC, Rodrigues CR, Loureiro NI, Castro HC, Lanfredi-Rangel A, Sabatini-Lopes J, Borges JC, Carvalho JM, Romeiro GA, Ferreira VF, Frugulhetti IC, Vannier-Santos MA (2006) Design, synthesis, SAR, and biological evaluation of new 4-(phenylamino)thieno[2,3-b]pyridine derivatives. *Bioorg Med Chem* 14(16):5765–5770. doi:10.1016/j.bmc.2006.03.013
12. dos Santos AE, Kuster RM, Yamamoto KA, Salles TS, Campos R, de Meneses MD, Soares MR, Ferreira D (2014) Quercetin and quercetin 3-O-glycosides from *Bauhinia longifolia* (Bong.) Steud.

- show anti-Mayaro virus activity. *Parasit Vectors* 7:130. doi:[10.1186/1756-3305-7-130](https://doi.org/10.1186/1756-3305-7-130)
13. Spindola KC, Simas NK, Salles TS, de Meneses MD, Sato A, Ferreira D, Romao W, Kuster RM (2014) Anti-Mayaro virus activity of *Cassia australis* extracts (Fabaceae, Leguminosae). *Parasit Vectors* 7:537. doi:[10.1186/s13071-014-0537-z](https://doi.org/10.1186/s13071-014-0537-z)
 14. Zhao L, Zhang Y, Dai C, Guzi T, Wiswell D, Seghezzi W, Parry D, Fischmann T, Siddiqui MA (2010) Design, synthesis and SAR of thienopyridines as potent CHK1 inhibitors. *Bioorg Med Chem Lett* 20(24):7216–7221. doi:[10.1016/j.bmcl.2010.10.105](https://doi.org/10.1016/j.bmcl.2010.10.105)
 15. Pevet I, Brulé C, Tizot A, Gohier A, Cruzalegui F, Boutin JA, Goldstein S (2011) Synthesis and pharmacological evaluation of thieno[2,3-*b*]pyridine derivatives as novel c-Src inhibitors. *Bioorg Med Chem* 19(8):2517–2528. doi:[10.1016/j.bmc.2011.03.021](https://doi.org/10.1016/j.bmc.2011.03.021)
 16. Galal SA, Abd El-All AS, Abdallah MM, El-Diwani HI (2009) Synthesis of potent antitumor and antiviral benzofuran derivatives. *Bioorg Med Chem Lett* 19(9):2420–2428. doi:[10.1016/j.bmcl.2009.03.069](https://doi.org/10.1016/j.bmcl.2009.03.069)
 17. Jakubowski A, Chlopicki S, Olszanecki R, Jawien J, Lomnicka M, Dupin JP, Gryglewski RJ (2005) Endothelial action of thienopyridines and thienopyrimidinones in the isolated guinea pig heart. *Prostaglandins Leukot Essent Fatty Acids* 72(2):139–145. doi:[10.1016/j.plefa.2004.10.011](https://doi.org/10.1016/j.plefa.2004.10.011)
 18. Karupiah G, Xie QW, Buller RM, Nathan C, Duarte C, MacMicking JD (1993) Inhibition of viral replication by interferon-gamma-induced nitric oxide synthase. *Science* 261(5127):1445–1448
 19. Bernardino AMR, Pinheiro LCS, Ferreira VF, Azevedo AR (2004) Synthesis and antiviral activity of new 4-(phenylamino)thieno[2,3-*b*]pyridine derivatives. *Heterocycl Commun* 10(6):407–410
 20. Bernardino AMR, de Azevedo AR, Pinheiro LCS, Borges JC, Carvalho VL, Miranda MD, de Meneses MDF, Nascimento M, Ferreira D, Rebello MA (2007) Synthesis and antiviral activity of new 4-(phenylamino)/4-[(methylpyridin-2-yl) amino]-1-phenyl-1H-pyrazolo [3,4-*b*]pyridine-4-carboxylic acids derivatives. *Med Chem Res* 16(7):352–369
 21. Baer A, Kehn-Hall K (2014) Viral concentration determination through plaque assays: using traditional and novel overlay systems. *J Vis Exp* 93:e52065. doi:[10.3791/52065](https://doi.org/10.3791/52065)
 22. Borenfreund E, Puerner JA (1985) Toxicity determined in vitro by morphological alterations and neutral red absorption. *Toxicol Lett* 24(2–3):119–124
 23. Reed LJ, Muench H (1938) A simple method of estimating fifty per cent endpoints. *Am J Epidemiol* 27(3):493–497
 24. Laemmli UK (1970) Cleavage of structural proteins during the assembly of the head of bacteriophage T4. *Nature* 227(5259):680–685
 25. Lipinski CA, Lombardo F, Dominy BW, Feeney PJ (2001) Experimental and computational approaches to estimate solubility and permeability in drug discovery and development settings. *Adv Drug Deliv Rev* 46(1–3):3–26 (pii: **S0169-409X(00)00129-0**)
 26. Ravichandran R, Manian M (2008) Ribavirin therapy for Chikungunya arthritis. *J Infect Dev Ctries* 2(2):140–142
 27. Elgizoli M, Dai Y, Kempf C, Koblet H, Michel MR (1989) Semliki Forest virus capsid protein acts as a pleiotropic regulator of host cellular protein synthesis. *J Virol* 63(7):2921–2928
 28. Patel RK, Burnham AJ, Gebhart NN, Sokoloski KJ, Hardy RW (2013) Role for subgenomic mRNA in host translation inhibition during Sindbis virus infection of mammalian cells. *Virology* 441(2):171–181. doi:[10.1016/j.virol.2013.03.022](https://doi.org/10.1016/j.virol.2013.03.022)
 29. Kanekiyo K, Hayashi K, Takenaka H, Lee JB, Hayashi T (2007) Anti-herpes simplex virus target of an acidic polysaccharide, nostoflan, from the edible blue-green alga *Nostoc flagelliforme*. *Biol Pharm Bull* 30(8):1573–1575 (pii: **JST.JSTAGE/bpb/30.1573**)
 30. Byrnes AP, Griffin DE (1998) Binding of Sindbis virus to cell surface heparan sulfate. *J Virol* 72(9):7349–7356